

# Variable Photon Energy Photoelectron Spectroscopy of Transition Metal Molecules

JENNIFER C. GREEN

*Inorganic Chemistry Laboratory, Oxford University, South Parks Road, Oxford OX1 3QR, U.K.*

Received November 29, 1993

## Introduction

When photons of sufficient energy interact with matter, ionization can occur with ejection of electrons. The energy of a photon is transferred to an electron, enabling it to overcome the forces binding it within a material, and giving it kinetic energy. The quantitative relationship between the incident photon energy,  $h\nu$ , and the kinetic energy of an ejected electron,  $E_k$ ,<sup>1</sup>

$$h\nu = I_k + E_k \quad (1)$$

gives an experimental method of determining binding energies,  $I_k$ , of electrons. A photoelectron (PE) spectrum, which is normally displayed as a plot of the number of electrons with a particular binding energy,  $N(E)$ , versus the binding or ionization energy, consists of a number of bands, giving direct evidence for the quantization of electron energies in chemical systems. The energies of the various PE bands give the energies of the ion states formed with respect to the ground state of the system and, consequently, with respect to each other. Turner<sup>2</sup> and Siegbahn,<sup>3</sup> in the 1960s, were the first to exploit the photoelectric effect for the direct investigation of electronic structure; their classic work underpins the field known variously as photoelectron spectroscopy (PES), photoemission studies of solids, and electron spectroscopy for chemical analysis (ESCA).

The simplest way of accounting for the number and type of ion states accessible on ionization is within the framework of molecular orbital (MO) theory. For a closed-shell molecule a primary ion state is expected for ejection of an electron from each occupied MO; thus a PE spectrum maps the MO structure of a molecule. Though it is well recognized that any quantitative calculation of ionization energies must involve modeling the excited-ion-state properties as well as those of a ground-state molecule, the simple association of a PE band with a hole in a formerly occupied MO is a powerful model for interpreting PE spectra and understanding trends in electronic properties and chemical reactivity.

In the field of transition metal chemistry the number of accessible ion states and associated PE bands gives rise to particular problems in assignment of PE spectra. Theoretical treatments of molecules of this size are not always sufficiently accurate to decide the ordering of ion states, and empirical methods of band assignment

have proved to be of particular value. A PE spectrum contains, as well as energy information, intensity information. Whereas ionization energies are independent of the photon energy employed, band intensities vary with photon energy, as was recognized early on by Price.<sup>4</sup> His pioneering use of both He I and He II photons (which have energies of 21.2 and 40.8 eV, respectively) for determination of PE spectra exposed various empirical rules which assisted ion-state assignment. With the advent of synchrotron sources providing continuous tunable radiation in the vacuum UV and soft X-ray region, more extensive studies of PE band intensities were possible.<sup>5</sup> This photon energy dependence of the intensities of bands in a PE spectrum, as well as its use in elucidating the electronic structure of transition metal molecules, is the principal concern of this Account.

## Photoelectron Cross Sections

The probability of photoionization to an ion state is termed a photoionization or photoelectron *cross section*, commonly denoted  $\sigma$ . In the experiments that are the subject of this Account, PE cross sections have been determined for gas-phase transition metal molecules using synchrotron radiation over a photon energy range of 15–120 eV. PE flux is a function of the angle of observation of the photoelectrons.<sup>6,7</sup> For example, for elliptically polarized light, such as is generated by a synchrotron source, the dependence of cross section on angle is given by the expression

$$\frac{d\sigma}{d\Omega} = \frac{\sigma}{4\pi} \left[ 1 + \frac{\beta}{4} (3P \cos 2\theta + 1) \right] \quad (2)$$

where  $\theta$  is the angle between the photoelectron trajectory and the polarization vector of the incident light and  $P$  is the degree of polarization. Measurements of band intensities are made at a "magic angle" where the intensity is independent of the angular parameter,  $\beta$ . The cross section is then directly proportional to the band intensity.<sup>8</sup> Direct photoionization is controlled by the dipole selection rule, but as a free electron can

(1) Einstein, A. *Ann. Phys.* 1905, 17, 132.

(2) Turner, D. W.; Al-Joboury, M. I. *J. Chem. Phys.* 1962, 37, 3007.

(3) Siegbahn, K.; Nordling, C.; Fahlman, A.; Nordberg, R.; Hamrin, K.; Hedman, J.; Johansson, G.; Bergmark, T.; Karlsson, S. E.; Lindgren, I.; Lindberg, B. J. *ESCA: Atomic, Molecular and Solid State Structure Studied by Means of Electron Spectroscopy*; Nova Acta Regiae Soc. Sci. Upsaliensis, Ser. IV: Upsala, 1967; Vol. 20.

(4) Price, W. C.; Potts, A. W.; Streets, D. G. In *Electron Spectroscopy*; Shirley, D. A., Ed.; North-Holland: Amsterdam, 1972.

(5) Eastman, D. E.; Freeouf, J. L. *Phys. Rev. Lett.* 1975, 34, 395.

(6) Schmidt, V. *Phys. Lett. A* 1973, 45, 63.

(7) Ghosh, P. K. *Introduction to Photoelectron Spectroscopy*; Wiley: New York, 1983.

(8) Manson, S. T.; Dill, D. In *The photoionization of atoms; Cross-Sections and Photoelectron Angular Distributions*; Brundle, C. R., Baker, A. D., Eds.; Academic Press: New York, 1978; Vol. 2, p 157.

Jennifer C. Green (née Bliham) was born in Tadworth, England, on December 30, 1941. She was educated at St. Hugh's College, Oxford, where she obtained her B.A., M.A., and D.Phil., the latter being supervised by Professor Jack Linnert and Dr. Peter Atkins. Her current post in Oxford is that of University Research Lecturer. Her research interests center around the electronic structure and bonding of transition metal compounds, and the relation between their electronic properties and their chemical reactivity. The main investigative tool used in these studies has been photoelectron spectroscopy.

assume any  $l$  value all one-electron photoionizations are allowed, and photoionization cross sections for particular ion states are all of the same order of magnitude. They vary with the photon energy used, and the variation is characteristic of the nature of the vacated orbital. In favorable circumstances, the photon energy dependence of a band's cross section is like the signature of the originating MO; the nature of that signature depends on the type of atomic orbitals that go to make up the MO. Thus, ideally, cross section studies can provide a firm basis for band assignment and also reveal details of molecular bonding.

The model on which most interpretations of molecular cross sections are based is that of Gelius.<sup>9,10</sup> It makes a simplifying assumption that the cross section for a MO is determined only by the cross section of the atomic orbitals constituting the MO. The one-electron cross section,  $\sigma_j$ , for the  $j$ th MO is given by eq 3. The summation is carried out over all the AOs,  $\chi_i^A$ , on the different atoms, A, which contribute to the MO,  $\phi_j$ . The

$$\sigma_j = \sum_{A,i} P_{j,i,A} \sigma_i^A \quad (3)$$

$\sigma_i^A$  are one-electron atomic cross sections, and the  $P_{j,i,A}$  are factors describing the weight of the contribution of the AOs to the MO. In a LCAO MO treatment they are given by the squares of the coefficients  $c_{j,i,A}$  of the AO  $\chi_i$  in the MO  $\phi_j$  (eq 4). The model is valid when the

$$P_{j,i,A} = (c_{j,i,A})^2 \quad (4)$$

contribution of the overlap electron density to the cross section is negligible and the effect of the anisotropy of the molecular ion potential on the outgoing electron wave function is small. Both these conditions are most likely to hold when the PE kinetic energy is high, and the cross section is dominated by the inner part of the wave function rather than the bonding region. At low photon energies molecular effects on ionization cross sections are well documented, but even in these regions atomic effects are evident and the Gelius model provides a good basis for molecular cross section interpretation.

Thus, in order to evaluate the photon energy dependence of molecular cross sections, we need to have a good appreciation of the range of atomic cross section variations. These latter are fairly well understood, and a useful compilation of calculated atomic cross sections for direct photoionization exists.<sup>11</sup>

In common with other electromagnetically induced electronic transitions, ionization probability can be shown to be proportional to the dipole matrix element,  $M_{if}$ , given in eq 5, where  $i$  represents the initial-state

$$|M_{if}|^2 = \sum_{i,f} |\langle f | r_\mu | i \rangle|^2 \quad (5)$$

wave function and  $f$  the final-state wave function.<sup>12,13</sup> In an orbital approximation this reduces to the interaction between the vacated orbital,  $\phi_i$ , and the photoelectron wave  $\epsilon_f$ . The interaction, and hence the cross section, will be largest when the vacated orbital and

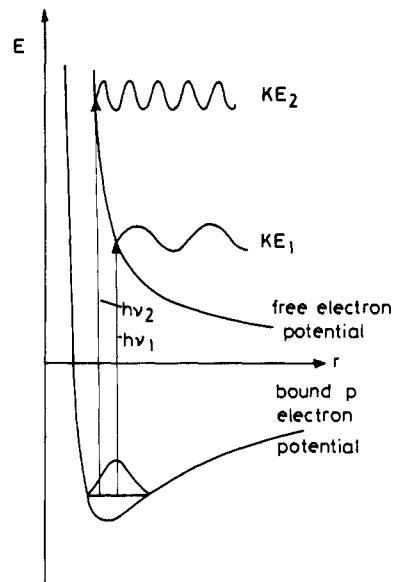


**Figure 1.** Representation of the wave function of an ionized orbital and a photoelectron wave of low kinetic energy and high kinetic energy showing that the nodal properties of the photoelectron wave are responsible for a decrease in cross section with photon energy.

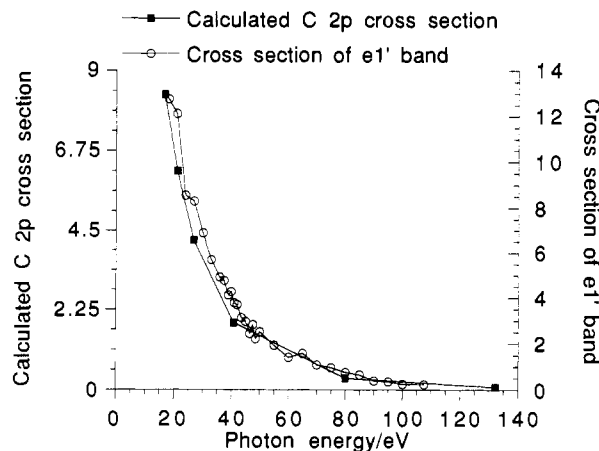


**Figure 2.** Cross section of the  $e_1'$  band of  $\text{Os}(\eta\text{-C}_5\text{H}_5)_2$  and a calculated cross section of a C 2p orbital.

the photoelectron wave are in the same spatial region. The magnitude is also dependent on the relative phases of the two wave functions.

A cross section is usually highest near the ionization threshold and after that decreases with increasing photon energy. As the kinetic energy of the photoelectron increases, its wavelength decreases and the electron wave becomes more oscillatory. As a consequence, the positive and negative parts of the dipole matrix element with the vacated orbital tend to cancel one another (Figure 1a-c), and the cross section suffers rapid decay. At very high photon energies,  $h\nu$ , the cross section should vary as  $\nu^{-3}$ . The rate of decay can be characteristic of the AO ionized; for example, H 1s orbitals decay more rapidly with photon energy than C 2p.<sup>11</sup>

A typical cross section decay is illustrated in Figure 2, which compares the experimentally measured cross section of a molecular orbital composed of C 2p orbitals (the  $e_1'$  band of  $\text{Os}(\eta\text{-C}_5\text{H}_5)_2$ ) with that calculated for a C 2p atomic orbital.<sup>11</sup> The scales are adjusted to enable a comparison of the rate of decay of the cross sections which are seen to correspond closely.

(9) Gelius, U.; Siegbahn, K. *Faraday Discuss. Chem. Soc.* 1972, 54, 257.

(10) Gelius, U. In *Electron Spectroscopy*; Shirley, D. A., Ed.; North-Holland: Amsterdam, 1972.

(11) Yeh, J. J.; Lindau, I. *At. Data Nucl. Data Tables* 1985, 32, 1.

(12) Manson, S. T. *Adv. Electron. Electron Phys.* 1976, 41, 73.

(13) Bates, D. R. *Mon. Not. R. Astron. Soc.* 1946, 106, 432.

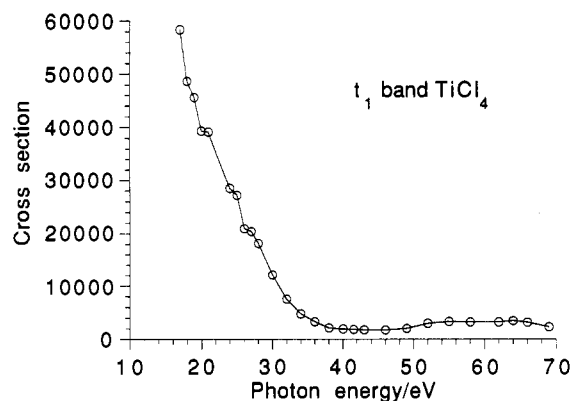


**Figure 3.** PE cross section of the  $t_1$  band of  $\text{TiCl}_4$  showing a Cooper minimum as a result of the radial node in the  $\text{Cl } 3p$  orbital.

Other variations superimposed on the decay can also be characteristic.

**Cooper Minima.** For orbitals with a radial node there is a minimum in the cross section, known as a Cooper minimum.<sup>14,15</sup> At some photon energy the contributions from the inner and outer parts of the orbital will tend to cancel one another. One example of the occurrence of such a minimum in the cross section of a transition metal compound is illustrated by the PE cross section of the  $t_1$  band of  $\text{TiCl}_4$  (Figure 3). The  $t_1$  orbital has, by symmetry, no metal contribution, so its ionization cross section results from its  $\text{Cl } 3p$  character. A  $\text{Cl } 3p$  orbital is calculated to have a Cooper minimum at a PE kinetic energy of 30 eV.<sup>11</sup> The kinetic energy of the photoelectron at the Cooper minimum of the  $\text{TiCl}_4$   $t_1$  orbital PE cross section is 34.2 eV. If an orbital has more than one radial node, there may be a corresponding number of Cooper minima in the cross section. The minima may occur just above threshold, as is the case for the  $3s$  orbital of  $\text{Na}$ ,<sup>11</sup> or at several hundred electronvolts, as is found for  $4d$  and  $5f$  electrons of transition elements.<sup>11</sup> Rules for Cooper minima have been arrived at by experimental and theoretical investigations: they only appear in  $l \rightarrow l + 1$  transitions; they occur only for outer and near outer subshells and only for those orbitals with radial nodes; and they are generally not zero minima because, even though the  $l \rightarrow l + 1$  dipole matrix element vanishes, the  $l \rightarrow l - 1$  one does not. The angular parameter,  $\beta$ , can vary substantially in the region of a Cooper minimum as the contribution from the  $l \rightarrow l + 1$  wave is small, leading to domination of  $\beta$  by the  $l - 1$  wave.

With such minima, the photon energy may be tuned to minimize the contribution from certain types of orbitals to a PE spectrum. Bancroft has used the Cooper minimum in the  $4d$  ionization of  $\text{Pd}$  to correct the assignment of the PE spectrum of  $\text{Pd}(\eta\text{-C}_3\text{H}_5)_2$ <sup>16</sup> and show that the ion-state ordering differs from that of  $\text{Ni}(\eta\text{-C}_3\text{H}_5)_2$ .<sup>17</sup>

The reduced rate of cross section falloff of the  $d$  bands of  $[\text{Cr}(\text{CO})_6]$  at high photon energy with respect to those of the equivalent bands of  $[\text{Mo}(\text{CO})_6]$  and  $[\text{W}(\text{CO})_6]$  is explained by the lack of a Cooper minimum in  $3d$  AO cross sections.<sup>18</sup> This is also found to be the case in the

(14) Cooper, J. W. *Phys. Rev. Lett.* **1964**, *13*, 762.

(15) Cooper, J. W. *Phys. Rev.* **1962**, *128*, 681.

(16) Li, X. R.; Bancroft, G. M.; Puddephatt, R. J.; Hu, Y. F.; Liu, Z.; Sutherland, D. G. J.; Tan, K. H. *J. Chem. Soc., Chem. Commun.* **1993**, 67.

(17) Li, X. R.; Bancroft, G. M.; Puddephatt, R. J.; Hu, Y. F.; Liu, Z.; Tan, K. H. *Inorg. Chem.* **1992**, *31*, 5162.

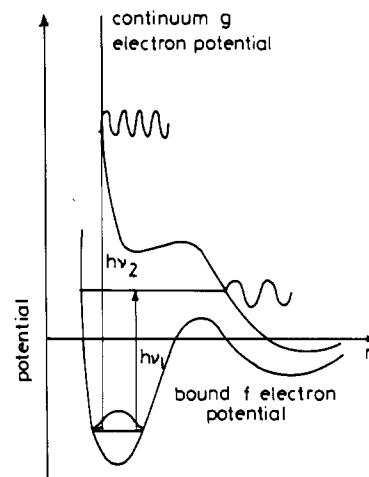


**Figure 4.** Representation of a bound  $f$  electron existing in the inner well region of its effective potential and low and high kinetic energy  $g$  free electron waves as possible ionization channels.

$d$  bands of ferrocene in comparison with its second- and third-row congeners.<sup>19</sup>

**Delayed Maxima.** Orbitals with high angular momentum, i.e.,  $d$  or  $f$  orbitals, often have maxima in their ionization cross sections some way above threshold. This is in contrast to  $s$  and  $p$  orbitals, where maxima, if they exist, tend to be very close to threshold. The effective potential experienced by an electron in an atom is given by the central field potential,<sup>20</sup> and the radial wave equation is given by eq 6.

$$\left[ -\frac{d^2}{dr^2} + \frac{l(l+1)}{r^2} + V(r) \right] \psi_{nl}(r) = E\psi_{nl}(r) \quad (6)$$

$V(r)$  is the Coulombic potential of the nuclei and other electrons, and  $l(l+1)/r^2$  is termed the centrifugal repulsion term and results from the solution of the angular part of the Schrödinger equation. For high values of  $l$ , the effect of the centrifugal term is to create a double well potential, which has an intermediate range maximum which may be positive. Figure 4 illustrates the case for a bound  $f$  electron which exists in the inner well escaping as a  $g$  electron wave. At low photon energies the ensuing wave has insufficient energy to penetrate the centrifugal barrier so the interaction between the  $f$  electron and the  $g$  wave is small. At higher photon energies the interaction improves and the cross section will pass through a maximum before decaying due to the normal oscillatory effects.

The ionization cross section of the  $f$  electrons of  $\text{U}(\eta\text{-C}_3\text{H}_5)_2$  (Figure 5) shows a delayed maximum at 39 eV.<sup>21</sup> Maxima in  $d$  electron cross sections tend to lie closer to threshold as the angular momentum is smaller. Nevertheless,  $d$  electron cross sections tend to increase, or decay rather more slowly than those of  $s$  and  $p$  electrons, between photon energies of 20 and 40 eV. As a consequence, changes in relative band intensity between He I and He II spectra can often be used in distinguishing between metal and ligand bands.<sup>22</sup>

**Resonant Enhancement of Cross Sections.** Perhaps the most dramatic departure from monotonic

(18) Cooper, G.; Green, J. C.; Payne, M. P.; Dobson, B. R.; Hillier, I. *J. Am. Chem. Soc.* **1987**, *109*, 3836.

(19) Cooper, G.; Green, J. C.; Payne, M. P. *Mol. Phys.* **1988**, *63*, 1031.

(20) Cowan, R. D. *The Theory of Atomic Structure and Spectra*; Chemical Abstracts Service: Columbus, OH, 1981.

(21) Brennan, J. G.; Green, J. C.; Redfern, C. M. *J. Am. Chem. Soc.* **1989**, *111*, 2373.

(22) Green, J. C. *Struct. Bonding* **1981**, *43*, 37.

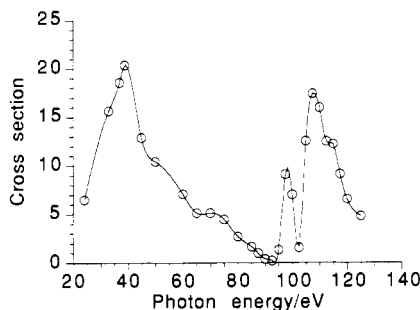


**Figure 5.** PE cross section of the 5f band of  $U(\eta-C_8H_8)_2$  showing a delayed maximum at 39 eV and 5d  $\rightarrow$  5f resonant enhancement of between 95 and 120 eV.

decay of a cross section occurs for d and f electron cross sections at photon energies near those necessary for excitation of particular core electrons. In these photon energy regions indirect ionization can occur, and such effects lie outside the calculations of Yeh. Indirect ionization may dominate the cross section in these regions; such occurrences are well exemplified by the cross sections found for ionization of the  $t_{2g}$  d electrons of the group 6 hexacarbonyls shown in Figure 6. Substantial structure is seen in the cross section plots of the  $nd$  electrons at and above the photon energy corresponding to the ionization energy of the core  $np$  electrons in the metal atom. Such massive variations in cross section do not come about as a result of direct interaction between the incident photon and the ionizing electron; rather they are the result of a two-stage process illustrated diagrammatically in Figure 7. Firstly the photon excites an electron from a core p orbital,  $\phi_c$ , to an empty d orbital,  $\phi_j$ . As a *resonance* process, allowed by the atomic selection rule of  $\Delta l = \pm 1$ , and occurring between two orbitals with the same principal quantum number which tend to occupy the same spatial region, this transition is highly probable and results in the ready uptake of a photon of appropriate energy by an atom or molecule. One possible mode of decay of the resulting highly excited state is for the electron to fall back into the hole in the core p shell and for another d electron, from orbital  $\phi_i$ , to be ionized. This second process is termed super Coster Kronig (SCK) decay. The probability of this process is proportional to the integral

$$\langle \phi_c | r_{\mu} | \phi_j \rangle \left\langle \phi_j \phi_i \left| \frac{e^2}{r_{12}} \right| \phi_c \chi_e \right\rangle \quad (7)$$

Again, a process such as this is most likely if all the orbitals involved occupy the same region of space; thus for excitation to an empty valence d orbital, it is most probable that a d electron is ionized and that the final hole is in the formerly occupied d orbital. It should be noted that the final state (c) is indistinguishable from that resulting from direct ionization of the d electron by the photon. Insofar as a PE experiment just detects the kinetic energy of the ejected electron, it cannot distinguish between the two processes and just records the variation in the band intensities.

Similar giant resonant enhancement of f electron cross sections is also found. In these cases resonant excitation is from a core  $nd$  orbital to an empty  $nf$  orbital, and SCK decay involves repopulation of the core d hole and ejection of an f electron. For example, the 5f band of  $U(\eta-C_8H_8)_2$  shows two resonant features at photon

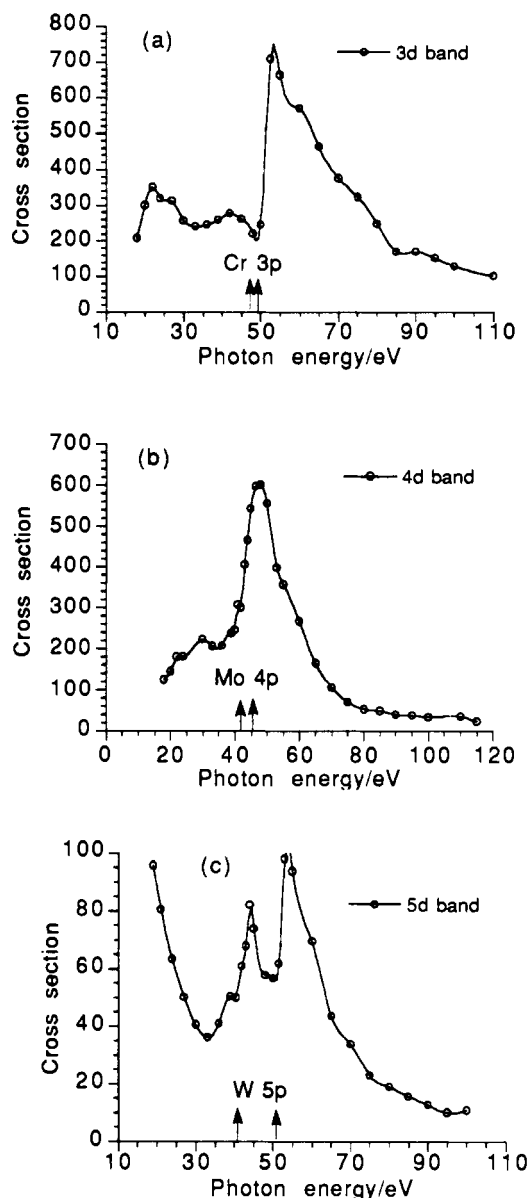


**Figure 6.** PE cross sections of the  $t_{2g}(d)$  ionization bands of (a)  $Cr(CO)_6$ , (b)  $Mo(CO)_6$ , and (c)  $W(CO)_6$ .

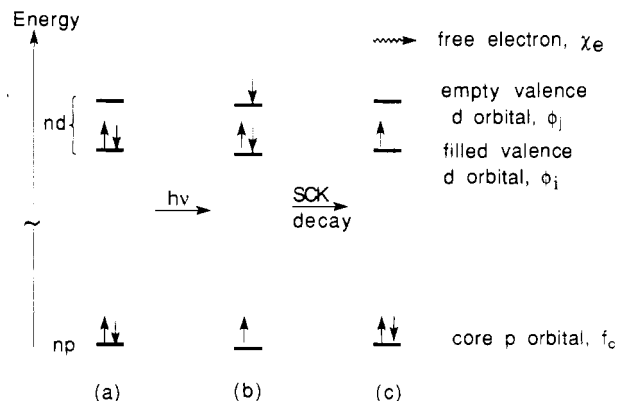


**Figure 7.** Diagrammatic representation of the processes underlying p  $\rightarrow$  d resonant enhancement of a d electron photoionization cross section: (a) initial state; (b) excited state after photoabsorption; (c) final state after SCK decay.

energies between 85 and 105 eV (Figure 5); these photon energies are sufficient to excite the 5d core electrons.

In the excited state, the excited electron has sufficient energy to leave the atom. For this state to exist long enough for SCK decay to be a possible fate, the excited

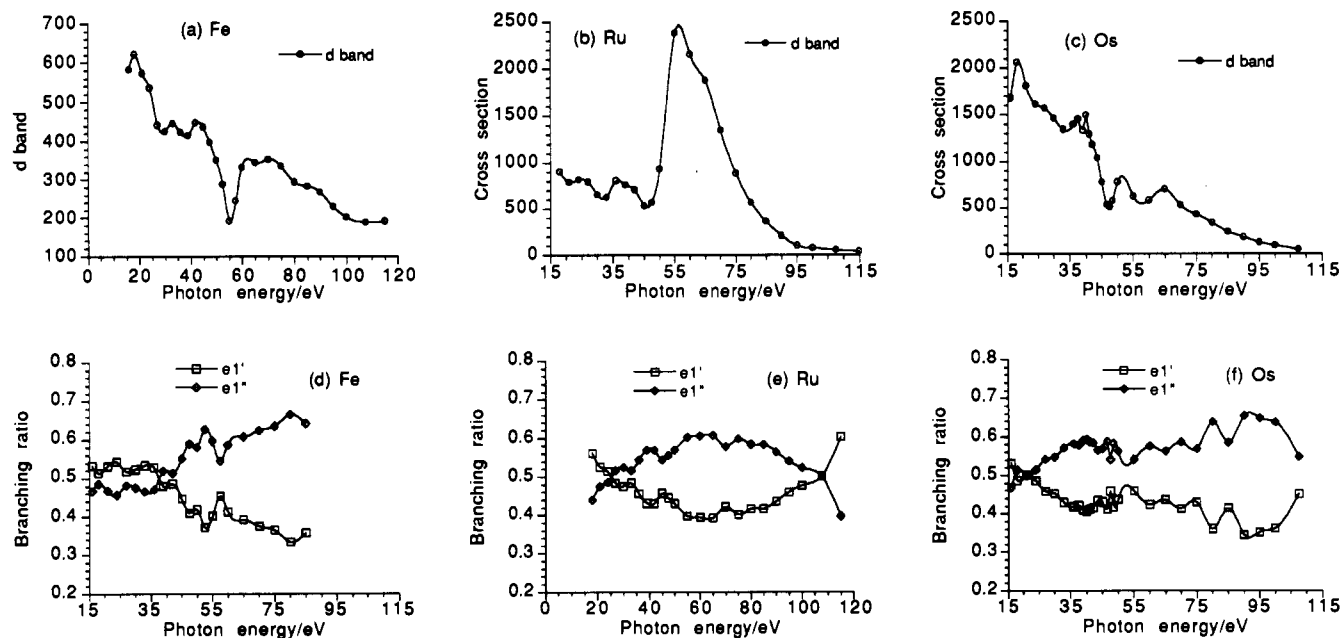


**Figure 8.** PE cross sections of the d bands of (a)  $\text{Fe}(\eta\text{-C}_5\text{H}_5)_2$ , (b)  $\text{Ru}(\eta\text{-C}_5\text{H}_5)_2$ , and (c)  $\text{Os}(\eta\text{-C}_5\text{H}_5)_2$  showing three different forms of Fano profile for the  $p \rightarrow d$  resonant enhancement of the cross section. Branching ratios of the  $e_1'$  and  $e_1''$  orbitals of group 8 metallocenes: (d)  $\text{Fe}(\eta\text{-C}_5\text{H}_5)_2$ ; (e)  $\text{Ru}(\eta\text{-C}_5\text{H}_5)_2$ ; (f)  $\text{Os}(\eta\text{-C}_5\text{H}_5)_2$ .

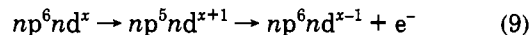
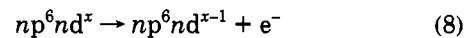
electron must be held momentarily within a potential barrier. Such barriers exist for high angular momentum electrons as has been explained above, and so these resonance features are found for d and f cross sections where the excited electron is trapped within such a centrifugal barrier, but not for s and p cross sections.

Such giant resonant enhancements of cross sections have several interesting features. It is apparent in the 5d cross section of  $\text{W}(\text{CO})_6$  (Figure 6) and the 5f cross section of  $\text{U}(\eta\text{-C}_5\text{H}_5)_2$  (Figure 5) that, for these heavier atoms, there are two maxima in the cross sections. These correspond to two different energies needed to promote the respective core electrons and can be accounted for by spin-orbit splitting of the resultant core hole state; the spin of the residual core electrons either reinforces or opposes their angular momentum. In the case of a 5p or 5d core hole the energy separation of the two states is sufficient to be resolved in the cross section plot. For the 4p and 3p core holes it is smaller and unresolved. In both the tungsten and the uranium cases, the two spin-orbit components of the resonance do not have the intensity ratio expected from the degeneracy of the hole states. For tungsten,  $P_{3/2}:P_{1/2}$  gives a ratio of 2:1, and for uranium,  $D_{5/2}:D_{3/2}$  gives a ratio of 3:2 with the higher angular momentum state at lower energy; in both cases it is the *higher* energy resonance that is the more intense. It has been shown that operation of the spin selection rules, which still influence the photoexcitation, can suppress transition to the lower energy hole states.<sup>18,21,23</sup>

The width of the cross section resonances is substantial, spreading over many electronvolts. Apart from the spin-orbit splitting mentioned above, for open shell systems exchange interaction between the core hole and the valence electrons can result in the spread of possible excited states over a wide energy range, many of which lie above threshold for the excited electron. In some solid-state examples, partial resolution of these states has been observed. Resolution of both spin-orbit and exchange couplings is made difficult by the

natural "line widths" resulting from the short lifetime of the excited state preceding SCK decay.

The cross section modifications resulting from the indirect ionization exhibit characteristic shapes known as Fano profiles.<sup>24,25</sup> These are a consequence of interaction of the two ionizing channels (eqs 8 and 9).



The electrons associated with each channel, as well as possessing energy, have phase. At the resonance threshold the two channels tend to be out of phase and the overall cross section decreases. At higher photon energies the two channels reinforce one another and ionization is augmented. The consequent increase in cross section depends on the relative strengths of the two channels. If the resonant channel is weak, enhancement may not occur and the resulting profile is seen more as a dip in the cross section. Three different types of profiles seem to be evident for the metallocene triad,  $M(\eta\text{-C}_5\text{H}_5)_2$ , where  $M = \text{Fe, Ru, and Os}$ . Their d band cross sections are shown in Figure 8. For Fe there is a dip in the cross section at 55 eV; for Ru strong enhancement is found with a small dip at 47.5 eV followed by a maximum at 55 eV; and for Os an intermediate situation exists with two minima at 47.5 and 60 eV and two weak maxima at 50 and 65 eV.

### Investigating Covalency

It was initially proposed that  $p \rightarrow d$  resonance enhancement of a cross section could only occur for d block transition metal compounds when the compound possessed both a d electron and a hole in the d shell,<sup>26</sup> the hole being necessary for initial promotion and the d electron for the SCK decay to be favored. In fact

(24) Fano, U. *Phys. Rev.* **1961**, *124*, 1866.

(25) Fano, U.; Cooper, J. W. *Phys. Rev. A* **1965**, *137*, 1364.

(26) Dehmer, J. L.; Starace, A. F.; Fano, U.; Sugar, J.; Cooper, J. W. *Phys. Rev. Lett.* **1971**, *1971*, 1521.

(23) Wendin, G. *Phys. Rev. Lett.* **1984**, *53*, 724.

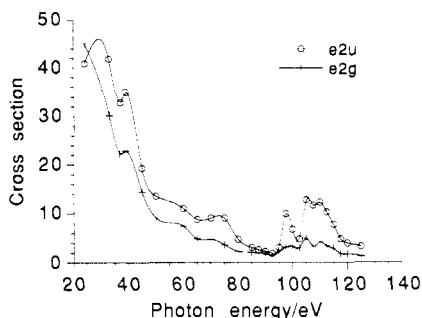


**Figure 9.** PE cross sections of the  $e_{2u}$  and  $e_{2g}$  bands of  $U(\eta-C_8H_8)_2$ ; compare with the cross section of the  $f$  band shown in Figure 4.

such resonant enhancement has been observed in PE cross sections for both  $d^0$  and  $d^{10}$  compounds. An example of the former is  $OsO_4$ <sup>27</sup> where the band associated with the  $1e$  and  $2t_2$  bonding electrons shows a pronounced double maximum in the cross section in the energy region associated with Os  $5p$  excitation. The two  $d$  bands of  $Ni(PF_3)_4$ ,<sup>28</sup> which possesses formally a complete  $d^{10}$  shell, both show a resonance in the photon energy region associated with Ni  $3p$  excitation (as does a region of the ligand bands). These results are readily understood if the covalent nature of the molecule is sufficient to introduce significant  $d$  content into what are regarded as principally ligand orbitals. In the case of  $OsO_4$  the  $1e$  and  $2t_2$  orbitals are calculated to have around 50% Os  $5d$  character. For  $Ni(PF_3)_4$  the LUMOs may have Ni  $3d$  character as a result of both P to Ni  $\sigma$  donation and Ni to P  $\pi$  back-donation. Excitation from the  $3p$  core to the LUMOs is therefore favored under atomic selection rules.

In favorable cases, therefore,  $p \rightarrow d$  and  $d \rightarrow f$  resonant enhancement of cross sections can be used to detect covalent interaction. A particularly striking example of this is in the investigation of  $U(\eta-C_8H_8)_2$ ,<sup>21</sup> which has three PE bands in the low IE region. The first band shows classic behavior for an  $f$  electron ionization with both a pronounced delayed maximum and two  $d \rightarrow f$  resonances (see Figure 5). The second and third bands are attributable to  $e_{2u}$  and  $e_{2g}$  ionizations arising from orbitals which are linear combinations of the ring  $e_2$  orbitals with possible contributions from the U  $6d$  and  $5f$  orbitals, respectively. The cross section variations of these two bands (see Figure 9) strongly suggest that the second comes from an orbital with  $5f$  content. Thus the second band is assigned to the  $e_{2u}$  ionization and the third to the  $e_{2g}$  ionization. Not only is  $f$  orbital covalency established for an actinide but the ordering of the ionization bands suggests that the  $6d$  orbitals are more effective at bonding than the  $5f$ .

The group 8 metallocenes,  $M(\eta-C_5H_5)_2$ , constitute another case where the  $d$  content of a bonding orbital, in these cases the  $e_1''$  orbital, can be investigated. As pointed out above, only in the case of  $M = Ru$  is the resonance in the  $d$  band cross section very strong, and it is only here that an analogous resonance is seen in the  $e_1''$  cross section. However, comparison of all the  $e_1''$  cross sections with those of the related  $e_1'$  orbitals, which can by symmetry have no  $d$  content, gives a clear

indication of  $d$  content in all three cases. The branching ratios (relative band intensities with respect to each other) of the two orbitals for all three compounds, shown in Figure 8, show that the initial decline in cross section is less for the  $e_1''$  orbital, that in the resonance region the  $e_1''$  band gains in intensity relative to the  $e_1'$  orbital, and that, in the case of  $M = Ru$  and  $Os$ , at photon energies approaching 100 eV there is a crossover in the branching ratio as the  $d$  orbital cross sections approach a Cooper minimum. All these pointers indicate  $d$  content in the  $e_1''$  orbitals for the three compounds.

There is another lesson to be learned from the  $Ru(\eta-C_5H_5)_2$  cross section investigation. Resonances are clearly visible also in other bands in the spectrum, though they are not as strong as in the main  $d$  band or as in the  $e_1''$  band. In the case of the  $e_1'$  band cross section, symmetry forbids any  $d$  content for the related orbital. The presence of a resonance, despite the lack of  $d$  content in the orbital, is accounted for by interchannel coupling, whereby final-state ionization channels mix and borrow intensity from one another. A classic example of this is in the PE spectrum of Xe where the extremely large xenon  $4d$  AO cross section in the region of its delayed maximum is mirrored by much smaller enhancements of the  $5s$  and  $5p$  cross sections.<sup>29</sup>

Thus it must be concluded that the absence of a  $p \rightarrow d$  resonance in a cross section does not necessarily mean no  $d$  character in the associated MO, and the presence of such a resonance does not necessarily mean the presence of  $d$  character. However, judicious assessment of relative resonant enhancements, together with examination of the total cross section pattern, can give strong evidence for  $d$  (and  $f$ ) orbital covalency.

### Shape Resonances

Though many of the features of molecular PE cross sections can be attributed to atomic effects, some features, such as shape resonances, can only be accounted for in molecular terms. Shape resonances<sup>30,31</sup> have no direct equivalent in atomic photoionization, being critically dependent upon the form of the potential of the molecular ion. This itself is determined in part by the physical shape of the molecule, from which the name of the effect derives. Shape resonances manifest themselves as increases in cross section, which are frequently sharp and generally at relatively low PE kinetic energies. They are generally viewed as attributable to momentary trapping of the valence orbital in a quasi-bound continuum orbital created by an effective potential of the molecular ion, or, excitation into antibonding orbitals located in the continuum.<sup>32</sup>

An alternative, though not incompatible, view of shape resonances is to regard them rather like EXAFS, where an ionizing electron is scattered from neighboring atoms, and so has maxima and minima in its amplitude as a function of its energy, as a result of the scattered waves reinforcing or interfering with the outgoing wave.

(29) West, J. B.; Woodruff, P. R.; Codling, K.; Houlgate, R. G. *J. Phys. B* 1976, 9, 407.

(30) Dehmer, J. L. In *Resonances in Electron-Molecule Scattering, van der Waals Complexes, and Reactive Chemical Dynamics*; Truhlar, D. G., Ed.; American Chemical Society: Washington, DC, 1984; Vol. 263.

(31) Dehmer, J. L. *J. Chem. Phys.* 1972, 56, 4496.

(32) Langhoff, P. W. In *Resonances in Electron-Molecule Scattering, van der Waals Complexes, and Reactive Chemical Dynamics*; Truhlar, D. G., Ed.; American Chemical Society: Washington, DC, 1984; Vol. 263.

(27) Green, J. C.; Guest, M. F.; Hillier, I. H.; Jarrett-Sprague, S. A.; Kaitsoyannis, N.; MacDonald, M. A.; Sze, K. H. *Inorg. Chem.* 1992, 31, 1588.

(28) Brennan, J. G.; Green, J. C.; Redfern, C. M.; MacDonald, M. A. *J. Chem. Soc., Dalton Trans.* 1990, 1907.

In this model also, it is apparent that the resonances are a function of the shape and size of the molecule.<sup>33</sup>

Maxima in the PE ionization cross sections of metallocenes and related sandwich molecules have been identified and assigned to shape resonances. The molecular potential for this series of molecules is expected to be very similar throughout the series and largely independent of the nature of the metal. For bis-cyclopentadienyl metal compounds a shape resonance occurs in a region between 36 and 40 eV,<sup>19</sup> whereas the  $p \rightarrow d$  resonances occur in the range 43–75 eV depending on the metal. Bis-arene<sup>34</sup> and cycloheptatrienyl-cyclopentadienyl compounds<sup>35</sup> show similar features. For the most part the shape resonances are most apparent in the metal-based orbitals, the strength of the resonance increasing with the metal character. An exception to this is the ionization cross section from the  $e_1'$  HOMOs of cobaltocene and nickelocene.<sup>36</sup> These antibonding  $d$  orbitals, with an extra radial node, show smaller  $p \rightarrow d$  resonances than the more metal localized  $a_1'$  and  $e_2'$  orbitals, in accord with the expectation of their respective metal characters, but significantly stronger shape resonances.

These and other instances of the presence of shape resonances and interchannel coupling in the region of 40-eV photon energy provide a cautionary note for the interpretation of relative increases in band intensity in He II spectra, compared to He I spectra, as attributable to metal  $d$  character. For example, such an increase in the fourth band in OsO<sub>4</sub> led to its assignment as a 5d-containing orbital, where the more extensive synchrotron study demonstrated it to originate from the  $a_1$  orbital, which by symmetry has no Os 5d character.<sup>27</sup>

### Quantifying $d$ Character

An obvious question is, To what extent can the presence of atomic effects in molecular cross sections be used to quantify the contribution of an atomic orbital to a MO? Inference from the Gelius model suggests that this should in theory be possible. Such an exercise is most likely to be profitable when the cross section behavior of the orbitals involved is strongly differentiated. That is often the case for organotransition metal molecules where the occurrence of delayed maxima,  $p \rightarrow d$  resonances, and Cooper minima (for 4d and 5f orbitals) all serve to distinguish  $d$  electron cross sections from those of C 2p orbitals. The presence of molecular effects such as shape resonances will, however, mitigate against such a quantification.

The study of the series of sandwich molecules  $M(\eta-C_7H_7)(\eta-C_5H_5)$ , where  $M = Mo, Nb,$  and  $Ta$ , provided a good opportunity to test whether such an approach could prove fruitful.<sup>35</sup> The  $a_1'$  ionization cross section may be taken as that of a pure metal  $d$  cross section, and the  $e_1$  ionizations may be taken as characteristic

of ring C  $p\pi$  orbitals. The  $e_2$  cross sections show behavior visibly intermediate between the two. A least squares fit of the  $e_2$  cross section to a linear combination of the other two cross sections was fairly successful, giving correlation coefficients of around 0.99. The deduced amounts of metal character on the ring  $e_2$  orbital were around 70% for Nb and Mo and 80% for Ta.

### Conclusions

The photoionization cross sections of  $d$  and  $f$  PE bands of gas-phase molecules show a number of characteristic features. These include maxima at relatively low photon energies due to centrifugal barrier effects, shape resonances, pronounced maxima and minima at photon energies corresponding to resonant absorption by inner shell electrons, and Cooper minima at high photon energies for ionization from  $d$  orbitals with radial nodes. These processes lead to cross sections for  $d$  and  $f$  ionization bands being highly structured. By contrast, cross sections of ionization bands from ligand-based orbitals are generally featureless and are characterized by a steep falloff at low photon energies followed by a less rapid decline. They may also display Cooper minima if the atomic orbital possesses a radial node, enabling distinction to be made, for example, between ionization from 2p and 3p orbitals. The cross section plots of ligand bands are thus strongly differentiated from those of  $d$  and  $f$  orbitals.

Establishment of these characteristic features has not only led to firm experimentally based band assignments but also to the demonstration of covalency in complexes, as orbitals with mixed metal-ligand character show cross section behavior which is a blend of that expected from the atomic constituents. In favorable circumstances a quantitative estimate of the metal  $d$  character of an MO may be achieved.

Though deductions of a similar nature are often made on the basis of just He I and He II spectra, they are not as reliable as when a more extensive photon energy range is employed owing to the prevalence of shape resonances in the low photon energy region.

Variable photon energy PE spectroscopy, which has now been applied to a wide variety of transition metal molecules, including coordination compounds,<sup>27,28,37–39</sup> organometallics,<sup>16–19,21,34,35,40</sup> metal-metal-bonded molecules,<sup>41</sup> and even quite large clusters,<sup>42</sup> considerably enhances the information content of a PE experiment and, with the wide availability of synchrotron sources, will influence the use of PE spectroscopy in the investigation of the electronic structure of transition metal compounds.

(37) Didziulis, S. V.; Cohen, S. L.; Gewirth, A. A.; Solomon, E. I. *J. Am. Chem. Soc.* **1988**, *110*, 250.

(38) Butcher, K. D.; Didziulis, S. V.; Briat, B.; Solomon, E. I. *J. Am. Chem. Soc.* **1990**, *112*, 2231.

(39) Butcher, K. D.; Gebhard, M. S.; Solomon, E. I. *Inorg. Chem.* **1990**, *29*, 2067.

(40) Yang, D. S.; Bancroft, G. M.; Puddephatt, R. J.; Tan, K. H.; N., C. J.; Bozek, J. D. *Inorg. Chem.* **1990**, *29*, 4956.

(41) Lichtenberger, D. L.; Ray, C. D.; Stepniak, F.; Chen, Y.; Weaver, J. H. *J. Am. Chem. Soc.* **1992**, *114*, 10492.

(42) Davies, C. E.; Green, J. C.; Kaltsoyannis, N.; MacDonald, M. A.; Qin, J.; Rauchfuss, T. B.; Redfern, C. M.; Stringer, G. H.; Woolhouse, M. G. *Inorg. Chem.* **1992**, *31*, 3779.

(33) Bozek, J. D.; Bancroft, G. M.; Cutler, J. N.; Tan, K. H.; Yates, B. W.; Tse, J. S. *Chem. Phys.* **1989**, *132*, 257.

(34) Brennan, J. G.; Cooper, G.; Green, J. C.; Kaltsoyannis, N.; Payne, M. P.; Redfern, C. M.; Sze, K. H.; MacDonald, M. A. *Chem. Phys.* **1992**, *164*, 271.

(35) Green, J. C.; Kaltsoyannis, N.; Sze, K. H.; MacDonald, M. A. *J. Am. Chem. Soc.*, in press.

(36) Brennan, J.; Cooper, G.; Green, J. C.; Payne, M. P.; Redfern, C. M. *J. Electron. Spectrosc. Relat. Phenom.* **1993**, *66*, 101.